Worst-case identification of touch voltage and stray current of DC railway system using genetic algorithm

C.S.Chang and L.F.Tian

Abstract: The problem of reducing the touch voltage and stray current in DC railways is multiobjective and conflicting. It is affected by many factors such as the earthing and bonding design, as well as the normal and failure operating conditions. An approach of genetic algorithm based multiobjective optimisation is proposed to identify the worst-case touch voltage and stray current in MRT systems. A two-step design scheme is formulated to represent both the normal and the failure conditions. The method of Pareto-optimal sets is developed to best improve the touch voltages and stray current integral for the normal condition. The decision-maker is given a powerful tool for picking the most appropriate earthing and bonding design from the set, and for identifying the worst-case performance from the list of credible failure conditions. Simulation results are presented which demonstrate the effectiveness of the proposed approach in fulfilling the design objectives.

List of principal symbols

TSS = traction substation
PS = passenger station
I_R = running rail current
I_S = stray current
I_T = train current
R_R = running rail resistance
R_S = earth resistance at passenger station
R_T = earth resistance at the train
F = objective functions
C = feasible set
$h(.)$ = equality constraints
$g(.)$ = inequality constraints
x = decision variables
x^* = non-dominated solution vector

1 Introduction

Mass rapid transit (MRT) power supply systems comprise three parts: the traction substations (TSSs), the go-circuit and the return-circuit. At TSSs, the AC supply voltage is stepped down and converted to DC. Catenary wires or third rails are used in the go-circuit. Running rails, rail bonds and return cables are the main components of the return circuit. Because of the rail-to-ground and rail resistances, there will be a voltage rise caused by the return current flows between the rails and the local ground known as the touch voltage. Excessive instantaneous touch voltages jeopardise safety. As running rails are usually lightly insulated, the traction current passing back to the substations may partly leak into the ground. The leakage current, known as stray current, is likely to be picked up by the

underground structures in the vicinity and cumulative stray current may accelerate their corrosion [1, 2].

The monitor and control of touch voltage and stray current is receiving increasing attention, while their computer simulation has been well studied. Since stray current causes accumulative corrosion proportional to the product of the magnitude of stray current and the time duration, the stray current used in this paper is represented by the stray-current integral collected from all earthing points. The touch voltage causes immediate harm and takes an instantaneous value.

To provide an accurate model of the stray-current integral, the peak loading condition should be studied. On the other hand, touch voltages tend to be highest under failure conditions. Unfortunately, improvement of either the stray-current integral or touch voltages tends to deteriorate the other. For instance, high rail-to-ground insulation is liable to present large touch voltages but small stray currents. To compromise between touch voltages and stray currents in identifying the worst-case solution, a two-step design procedure is proposed, as in Fig. 1.

In Step 1, the algorithm extensively explores several earthing and bonding arrangements under normal operation. The method of Pareto-optimal sets is used to obtain a set of optimal solutions of the bicriterion optimisation problem. In each solution, the earthing and bonding design is optimised to best improve the two criteria of touch voltages and stray-current integral. Each solution therefore represents a different degree of trade-off between the two criteria.

The Pareto-optimal set from step 1 contains a large collection of optimal designs. This is also a source of reference for different design variations. Because the specific times at which initiating events that cause failure condition are unpredictable, any optimal design taken from step 1 must be operated at all times in such a way that the system will not be endangered should any credible failure occur. In step 2, the decision-maker picks one optimal design from the set, and performs a performance check with the list of credible failure conditions. The worst-case touch voltages and stray-current integral are identified during checking.

570

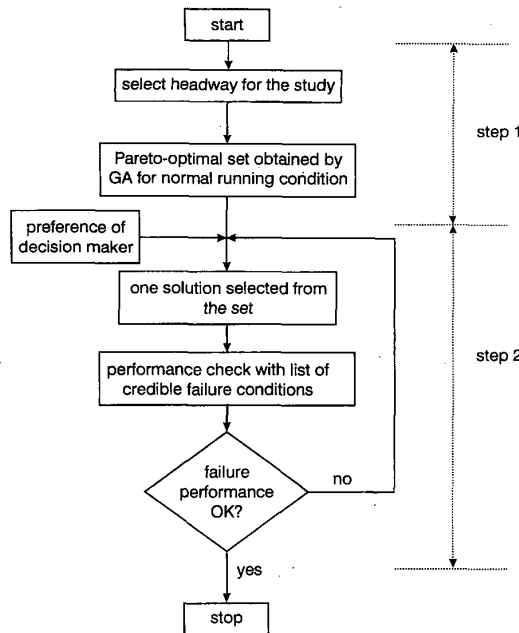*IEE Proc.-Electr. Power Appl., Vol. 146, No. 5, September 1999*

Fig. 1 *Overall layout of two-step design procedure*

The decision-maker prepares his/her own list of credible failures from predefined events such as substation out-of-service, broken or deteriorating bonding and joints, etc. Should the worst case be unsatisfactory, the decision-maker is prompted to pick another optimal design from the set for a further performance check.

2 Multiobjective optimisation of earthing and bonding design for normal operation

In a general multiobjective optimisation, the vector $F(x)$ contains a set of objective functions $f_i(x)$, uniquely defined by the set of variable x. $F(x)$ is to be minimised (or maximised) individually:

$$\min_{x \in C} F(x) = [f_1(x), f_2(x), \dots, f_n(x)]$$

$$\text{subject to } C = \{x : h(x) = 0, g(x) \le 0\} \qquad (1)$$

where n (= 2 in this problem) defines the number of objective functions in the vector $F(x)$. C denotes the feasible set of x, which is subjected to equality and inequality constraints.
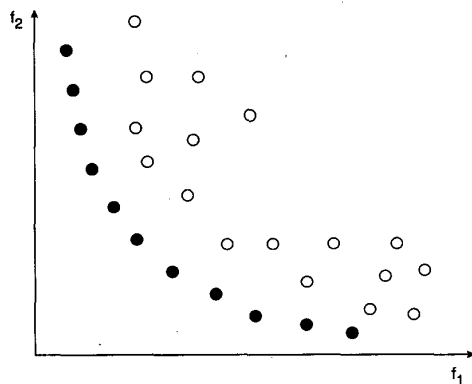

Fig. 2 *Pareto front for bicriterion minimisation problem*
● non-dominated solutions
○ dominated solutions

Feasible solutions to the above multiobjective optimisation problem are known as non-dominated solutions in a Pareto-optimal set. Each solution is uniquely defined by a parameter vector $x^* \in C$. To qualify as a non-dominated solution, a solution should not be dominated by any other solutions, i.e. there is no $x' \in C$ such that $f_i(x') \le f_i(x^*)$ for all $i = 1, 2, \dots, n$, and $f_j(x') < f_j(x^*)$ for some $j = 1, 2, \dots, n$.

Fig. 2 shows all the possible (dominated and non-dominated) solutions of a bicriterion optimisation problem for $f_1(x)$ and $f_2(x)$, where all non-dominated solutions are situated on a circular arc known as a Pareto-optimal front. Solution points, which are not situated at the front, are dominated solutions and are discarded during the optimisation (see Appendix).

2.1 Optimisation variables

Touch voltages and stray currents are affected under normal condition by factors such as the passenger substation spacing, rail resistance and rail conditions, headway interval, synchronisation delay, weather condition, soil resistivity, and earthing and bonding design. Among these factors, a close TSS spacing decreases the go-circuit voltage drops, but the spacing is determined by other considerations such as the ease of construction and commercial benefit [3]. Once the MRT system is designed, the rail resistance is fixed and cannot be changed easily. The headway depends on the passenger traffic flow. It usually takes constant values during certain periods, e.g. rush hours, normal hours and evening hours. The synchronisation delay varies during the actual train run from zero to the headway specified at the time. The touch voltage and stray current are also affected by operational abnormality (or failure), which can be the result of track paralleling switched off, substations out of service, etc. In our work, the earthing and bonding arrangement is first optimised against the normal-condition factors.
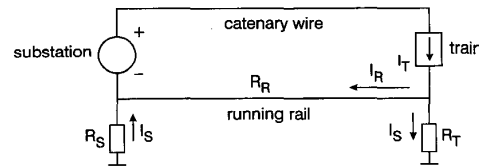

Fig. 3 *Simple case study of touch voltage and stray current*

A simplified single-TSS and single-train model is shown in Fig. 3. The stray current of this model is

$$I_S = \frac{R_R I_T}{R_T + R_R + R_S} \qquad (2)$$

where I_T is the train current, R_R is the running rail resistance, R_S is the earth resistance at the TSS, and R_T is the earth resistance as seen at the train.

In eqn. 2, the train current I_T is largely affected by the train schedule and passenger flow [4]. Loadflow studies using the train current simulate the performance, voltage profile and harmonic distortion of the go-circuit, as well as the contribution of power from each TSS. As the running rail resistance R_R is decided at the design stage of the MRT system, R_S and R_T are the only variables to be investigated. In general, low R_S and R_T give rise to a high stray current but a relatively low rail potential. Regular bonding of the rails equalises the rail-to-earth potentials of all rails along the return circuit. It also reduces the return resistance because of parallel rail paths constituting the return-circuit. The earthing and bonding arrangement is hence chosen as the decision variables in step 1, and optimised to best improve the touch voltages and stray currents.

2.2 Approaches of multiobjective optimisation

In traditional methods of multiobjective optimisation, different criteria are linearly blended into a composite scalar objective. This requires pre-establishment of the weights of different criteria. However, in many cases, the utility function is not known prior to the optimisation problem. As there is usually no common metric between different criteria, the weighted combination is difficult. On the other hand, differently weighted combinations lead to different results because different parts of the information are emphasised. The solution using one set of weights provides only one of the Pareto-optimal solutions, as in Fig. 2. As it is never a simple task to specify an appropriate set of weights, optimal solutions are individually obtained for a range of weights and the so-called trade-off curves are generated [5]. The computing time required for generating the trade-off curves is high and it is difficult to apply such techniques to non-convex problems.

The concept of a Pareto-optimal set is therefore introduced into step 1 to eliminate the problem as above. In this, each objective function is utilised separately rather than collectively. The parallel search characteristic of the GA makes it possible to solve the multiobjective optimisation efficiently. Such a GA feature is exploited in this work to formulate effective selection and reproduction operators to generate the Pareto-optimal set. Pioneering work was carried out by developing the vector evaluated genetic algorithm for multiobjective optimisation [6]. In the algorithm, the non-commensurable objective functions are treated independently. The population in the current generation is divided into sub-populations based on each of the objectives separately to reproduce the next generation. In the population-based but non-Pareto approaches, the generated candidate solutions give satisfactory results at only one objective but perform poorly at the other objectives. Their performances are somewhat similar to that of weighting objective function optimisation. In contrast to the vector evaluated genetic algorithm, the Pareto-based approach is to process selection and reproduction on the basis of not only the objective values themselves, but also their dominance properties. All the locally non-dominated points achieve equal reproductive potential through a non-dominated sorting procedure. In [7], a method is proposed for rank assignment according to the Pareto-optimality of an individual, which is explained in detail in the Appendix. This method tries to trace all the non-dominance individuals in the present population as far as possible. When all the non-dominated individuals in the current generation are picked, the recombination operators are then applied to produce the next generation. The above procedure is iterated to locate the Pareto-optimal points and produce subsequent populations until the convergence condition is met. The final non-dominated set represents the collection of trade-off solutions among all the objectives.

The proposed scheme follows the general outline of the Pareto-based approach as described above. The conventional genetic algorithm (GA) is, however, modified as in the Appendix to deal with the present multiobjective problem.

3 Return circuit simulation

As in Fig. 4, the MRT system studied in this paper has two tracks. There are 16 passenger stations, 7 of which are chosen as TSSs. The trains are provided with regenerative braking and dispatched in either the UP- or DN-direction. The passenger stations are located at an interval of 1~2 km. At each passenger station, the pair of running rails carrying

each train are bonded (known as cross bonding) to reduce the impedance of the return circuit. However, the pair of running rails has the option of being bonded to the other pair of running rails in the opposite direction (interbound bonding). Since all trains are dispatched with the same pre-specified headway and synchronisation delay, it is sufficient to use the headway interval as the period of the optimisation [3]. The time step of simulation is taken as one second. Moreover, it is assumed that the stray current path resistance, which changes with many practical factors, is known and can be varied later for scenario studies. The flowchart of the return-circuit simulation is illustrated in Fig. 5. The train movement module is first run to obtain the speed–distance profile and the current–distance profile. The AC/DC load flow is then applied to calculate the train currents and TSS currents in the go-circuit. Using these currents, a second network solution is applied to the return-circuit to calculate the touch voltage and stray current.
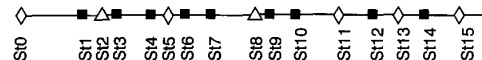
Fig. 4 *Layout of MRT system*
■ passenger station
△ traction substation (rectifier only)
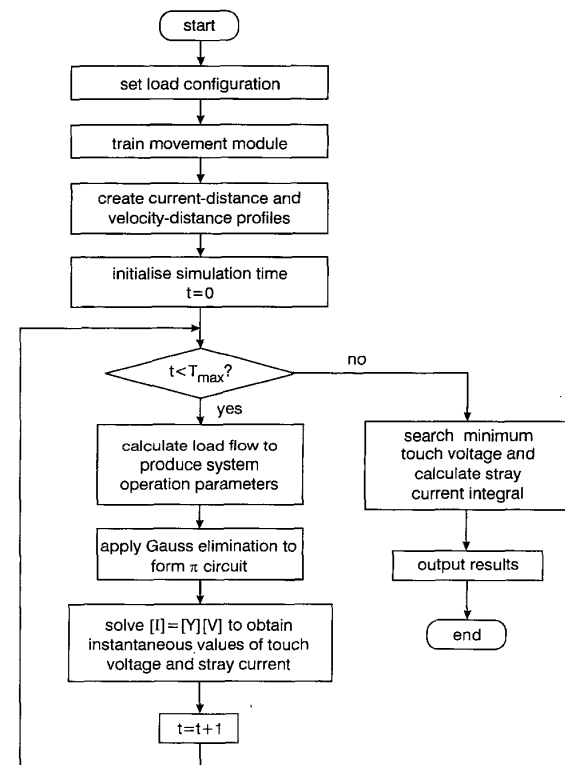◇ traction substation (rectifier and inverter)

Fig. 5 *Flowchart of return-circuit simulation*

Like the AC/DC loadflow in the go-circuit, the load referral method [4] is used to remove the train nodes from the return-circuit model. Thus, only the network nodes are retained as the circuit nodes, and the dimension of the return-circuit model is fixed at a small value. Without the use of the load referral method, the dimension of the model is time varying. The return system is modelled accurately with 15 equivalent π circuits with nonlinear representations of running rails, earthing and ground resistances, etc.

MRT systems have been provided with either total floating, direct earth or diode earth. The return-circuit

572

Table 1: Typical arrangements of earthing and bonding

Simulation no.	Simulation condition	Positive touch voltage, V	Negative touch voltage, V	Stray current integral, Ah
1	As default	74.13	–80.75	41.62
2	All PSs direct earth, bonding as default	67.04	–78.83	156.94
3	All PSs diode earth, bonding as default	98.34	–58.53	83.10
4	All PSs interbound bond, earthing as default	74.11	–80.64	41.84
5	All TSSs direct earth, bonding as default	77.49	–76.55	82.78
6	All TSSs diode earth, bonding as default	93.91	–61.66	67.31
7	All TSSs interbound bond, earthing as default	74.14	–80.59	41.84
8	All PSs direct earth & interbound bond	78.03	–65.74	202.85
9	All PSs diode earth & interbound bond	98.20	–57.82	83.02
10	All TSSs direct earth & interbound bond	87.79	–63.94	107.55
11	All TSSs diode earth & interbound bond	93.81	–57.82	67.36
12	All TSSs direct earth and all PSs diode earth, bonding as default	85.55	–70.05	104.01
13	All TSSs diode earth and all PSs direct earth, bonding as default	74.61	–70.01	150.34
14	All TSSs interbound bond and all PSs direct earth	64.80	–83.36	117.56
15	All TSSs interbound bond and all PSs diode earth	90.97	–69.47	62.78
16	All TSSs direct earth and all PSs interbound bond	77.41	–76.72	82.89
17	All TSSs diode earth and all PSs interbound bond	93.83	–60.54	67.36

As a default, all TSSs and PSs are not provided with interbound bonding and are floating

simulation allows a mix of different earthing arrangements at either the TSSs or passenger stations (Section 4). To take the cumulative effect of stray current into account, the total integral stray current collected for all earthing points as defined in [8] is employed in this paper.

4 Optimisation results

To gain insight, simulations are carried out on the study MRT system for a. variety of earthing and bonding arrangements. The touch voltages and the total integral stray currents collected for all earthing points listed in Table 1 have exhibited certain patterns of variations for the earthed and unearthed arrangement. Generally speaking, both the touch voltage and the average stray current tend to increase when the headway is decreased. The headway used in this study is 180s, which is the headway used during the peak hours. Floating the return pole is seen to reduce the stray current to roughly half, as compared to a solidly earthed arrangement. The floating arrangement does, however, raise concerns about touch voltage and makes the low-level stray current difficult to detect and clear. The bonding of rails provides adequate path for the return traction current, decreases the mutual resistance, and thus increases the traction current in the return path.

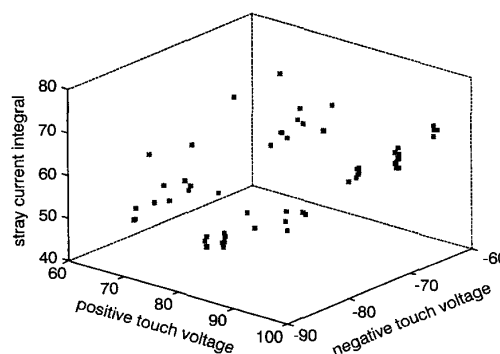### 4.1 Multiobjective optimisation for normal condition

To best improve the touch voltages and stray-current integral, the proposed approach is executed to optimise the three objectives: the maximum positive touch voltage (f_1), the minimum negative touch voltage (f_2), and the total integral stray current collected for all earthing points (f_3). f_2 is chosen due to the unidirectional characteristics of the diode earth.

The proposed multiobjective optimisation is carried out for two configurations:

(i) Configuration 1: earthing and bonding taken at all TSSs only

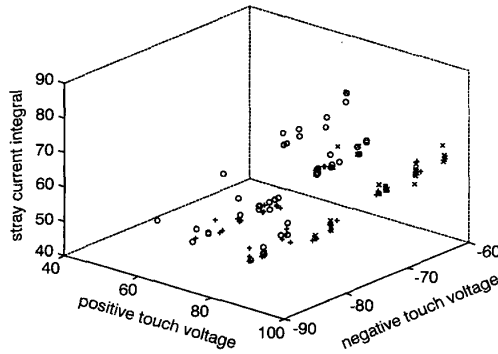(ii) Configuration 2: earthing and bonding taken at all passenger stations (PSs)

Since the study MRT system has 16 passenger stations, a GA string of 48 bits (16 × 3-bit substrings) is formed for configuration 2 to represent the earthing and interbound bonding at all 16 passenger stations. It is assumed that all passenger stations are cross-bonded (Section 3). Each substring consists of 3 binary bits. The first 2 bits are used for identifying the earthing strategy, which can be floating, directly earthed or diode earthed. The last bit is set to either one or zero to provide interbound bonding at each passenger station or not. Likewise, the GA uses a string of 21 bits for the 7 TSSs in configuration 1. The computer program for the optimisation of touch voltage and stray current is written in Visual C++. The program typically takes 50min for the optimisation with a generation number of 5 and a population of 100.
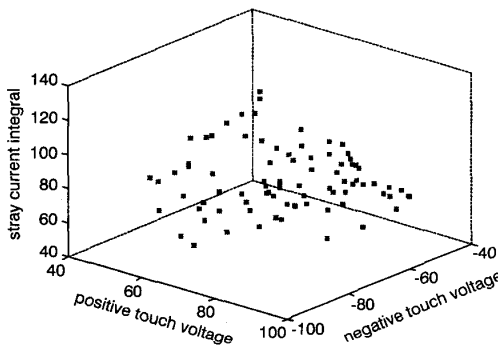

Fig. 6 *Pareto-optimal set for configuration 1: equal priority assigned to minimum touch voltages and stray current integral*

As shown in Figs. 6–9, the decision-maker is presented with four Pareto-optimal sets, which contain the solutions with equal and different priorities for configuration 1 and configuration 2. The solutions contained in each set represent a different trade-off among the three objective func-
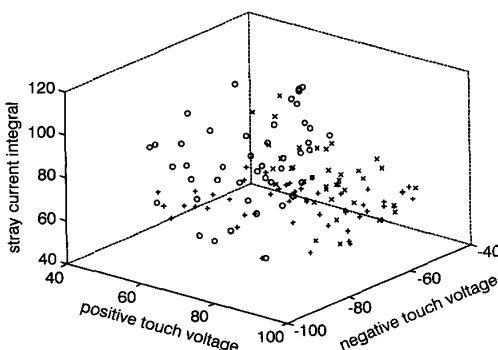
IEE Proc.-Electr. Power Appl., Vol. 146, No. 5, September 1999

573

tions. If the positive touch voltage (f_1) takes priority over the other two objectives, then more solutions ('○' in Figs. 7 and 9) gather in the region of small positive touch voltage values. A similar observation is made if priority is assigned to the other two objectives. From Figs. 7 and 9, three extreme solutions are picked from the vertices of the plots for configuration 1 and configuration 2. Tables 2 and 3 each contains the three extreme solutions together with a well-balanced solution with equal priority on the three objectives.

Fig. 7 *Pareto-optimal set for configuration 1: different priorities assigned to minimum touch voltages and stray current*
○ positive touch voltage has highest priority
× negative touch voltage has highest priority
+ stray current integral has highest priority

Fig. 8 *Pareto-optimal set for configuration 2: equal priority assigned to minimum touch voltages and mean stray current*

Fig. 9 *Pareto-optimal set for configuration 2: different priorities assigned to minimum touch voltages and stray current*
○ positive touch voltage has highest priority
× negative touch voltage has highest priority
+ stray current integral has highest priority

By comparing the four solutions in Table 2 with the four solutions in Table 3, configuration 2 appears to carry higher stray currents (f_3) than configuration 1. The former has, however, out-performed the latter from the point of

view of both f_1 and f_2. This appears reasonable as the former provides more earthing and bonding locations. Since both configuration 1 and configuration 2 are optimised, the solutions in Tables 2 and 3 have out-performed the typical cases in Table 1.

Table 2: Multiobjective optimisation of earthing and bonding for configuration 1

Solution	Priorities on f_1, f_2 and f_3	Lowest positive touch voltage, V	Lowest negative touch voltage, V	Lowest stray current integral, Ah
1.1	same priority for all	64.83	−60.26	42.89
1.2	highest priority on f_1	59.52	−64.79	41.80
1.3	highest priority on f_2	73.12	−60.19	47.57
1.4	highest priority on f_3	64.81	−61.55	41.81

f_1 is the positive touch voltage; f_2 is the negative touch voltage; and f_3 is the stray current integral

Table 3: Multiobjective optimisation of earthing and bonding for configuration 2

Solution	Priorities on f_1, f_2 and f_3	Lowest positive touch voltage, V	Lowest negative touch voltage, V	Lowest stray current integral, Ah
2.1	same priority for all	53.28	−57.57	51.38
2.2	highest priority on f_1	53.20	−65.80	47.90
2.3	highest priority on f_2	67.44	−56.37	52.41
2.4	highest priority on f_3	58.10	−56.10	47.58

f_1 is the positive touch voltage; f_2 is the negative touch voltage; and f_3 is the stray current integral

Table 4: Performance check of case 2.1 with list of credible failure conditions

Failure	Substation outage	Positive touch voltage	Negative touch voltage	Stray-current integral	Lowest train voltage
1	None	53.28	−89.41	86.92	1213.0
2	St0 1Rec	55.53	−91.18	87.49	1212.0
3	St2 1Rec	66.89	−95.6	90.72	1153.3
4	St5 1Rec	62.32	−103.46	95.04	1151.1
5	St8 1Rec	63.54	−104.1	102.38	1128.1
6	St11 1Rec	53.23	−94.06	92.05	1163.7
7	St13 1Rec	55.51	−82.89	88.71	1205.2
8	St15 1Rec	53.28	−89.41	87.39	1211.2
9	St0 2Rec	53.28	−83.74	92.91	1216.2
10	St0	95.35	−107.78	94.65	1080.4

4.2 Performance check for failure conditions

Table 4 shows the performance checks on a well-balanced solution of configuration 2 as listed in the first row of Table 3. The list of ten credible failure conditions is given in the second column. Almost all three objectives have deteriorated drastically due to outage of a TSS or a rectifier at TSS.

5 Conclusions

A multiobjective optimisation approach is proposed in this paper to identify the worst-case touch voltage and stray

574

current in MRT systems. As the results are affected by both the normal condition and failure conditions, a two-step solution scheme has been formulated to represent both conditions. The method of Pareto-optimal sets has been developed to best improve the touch voltages and stray-current integral for the normal condition. Care has been taken to ensure a comprehensive and uniform spread of optimal solutions within the set. The decision-maker is given a powerful tool for picking the most appropriate earthing and bonding design from the set, and for identifying the worst-case performance from the list of credible failure conditions.

6 References

1 SUNDE, E.D.: 'Earth conduction effects in transmission systems' (Dover Publication Inc., 1968)
2 JACIMOVIC, S.D.: 'Maximum permissible values of step and touch voltages with special consideration to electrified railroads', *IEEE Trans. Ind. Appl.*, 1984, **IA-20**, (4)
3 CHANG, C.S., LOW, J.S., and SRINIVASAN, D.: 'Application of tabu search in optimal design and operation of MRT power supply system', *IEE Proc., Electr. Power Appl.*, 1999, **146**
4 CHANG, C.S., CHAN, T.T., and LEE, K.K.: 'Network switching and voltage evaluation using an expert system in AC railway systems', *IEE Proc. B, Electr. Power Appl.*, 1992, **139**, (1)
5 CHANG, C.S., WANG, W., LIEW, A.C., and WEN, F.S.: 'Bicrite-rion optimisation for traction substations in mass rapid transit systems using genetic algorithm', *IEE Proc., Electr. Power Appl.*, 1998, **145**, (1), pp. 49–56
6 TAMAKI, H., KITA, H., and KOBAYASHI, S.: 'Multi-objective optimisation by genetic algorithms: a review'. IEEE international conference on *Evolutionary computation*, Japan, 1996
7 GOLDBERG, D.E.: 'Genetic algorithms in search, optimisation, and machine learning' (Addison-Wesley, 1989)
8 YU, J.G.: 'The effects of earthing strategies on rail potential and stray currents in DC transit railways'. Proceedings of international conference on *Developments in mass transit systems*, London, 1998

7 Appendix: Genetic algorithm based multiobjective optimisation

7.1 Review of genetic algorithm

The GA was motivated by ideas from natural genetics, and has been successfully applied to a variety of optimisation problems. The GA starts with a population of chromosomes and the abstract representations of candidate solutions. Evaluations of chromosomes in the current generation are based on the problem-dependent fitness function. Chromosomes with higher fitness are selectively picked for reproduction. By employing crossover and mutation, a low probability operator and a high probability operator, respectively, information encoded in these selected chromosomes is recombined. Successive populations are generated to form the subsequent generation. In this way, the GA attempts to find all the optima in the search space and realise the Darwinian notion of competitive evolution. The fittest members of the population would survive, as their information content is preserved, combined and evolved to produce even better offspring.

7.2 Modified genetic algorithm with fitness sharing

Conventional GAs suffer from the inherent drawback of genetic drift [7], which forces all candidate solutions into a few clusters rather than uniform scatter along the Pareto front, as in Fig. 2. To overcome such a problem, a niche mechanism of fitness sharing is specifically developed at the phenotypic level to maintain the solution diversity. Through dividing the populations into different niches, each peak and its neighbourhood receives a fraction of the population related to its height. In addition, the fitness of each candidate solution is reduced by an amount proportional to the density of candidate solutions present in its

neighbourhood. The convergence occurs within a niche rather than within the full population. Therefore, a uniform spread of non-dominant points for multiobjective optimisation problems is obtained along the Pareto-optimal front.

7.3 Selection processing with rank assignment

While retaining the same concept of crossover and mutation as the conventional GA, the proposed approach exerts a degree of control over the selection process by applying the rank assignment method as proposed in [7] for the multiobjective problem. During the present GA evolution, candidates in the current generation are compared by considering the following Pareto-optimality conditions, and ranked to decide on their chances of survival in the next generation. First, all the non-dominated candidates in the current generation are identified as rank 1 and marked. Then the non-dominated candidates among the unmarked solutions are ranked as 2 and marked. The above rank assignment procedure is repeated recursively as in Fig. 10, until the current rank number reaches a pre-specified value or the size of the unmarked population becomes smaller than a certain value. Afterwards, those candidates with a favourable rank (say, less than 6) survive, whereas candidates with a rank higher than the threshold (greater than 6) are discarded. The preserved candidates are then selected and recombined to produce the subsequent generations. Meanwhile, the non-dominated candidates among the preserved ones are recorded in the Pareto solution set. Each time a non-dominated solution is generated, the set of existing Pareto solutions will be updated. If any member in the set of Pareto solutions does not dominate the new non-dominated candidate, this candidate will be added to the set. On the other hand, any solution in the set that is dominated by the added point will be eliminated from the set. Therefore, at the end of GA evolution, the set of Pareto solutions comprises only non-dominated candidates generated during the whole evolution procedure.

```
Generate initial population P(0);
Evaluate P(0);
t:=0;
repeat
    Generate P(t+1) using P(t) as follows
    {  Assign ranks to the individuals in the P(t) as follows
        {  rank_value:=1;
           repeat
               Find all the non-dominated ones among all the un-visited individuals;
               Assign their ranks to be rank_value;
               Set visit flag to the assigned individuals;
               rank_value:= rank_value+1;
           until the rank_value is equal to the set value or all the individuals are visited
        }
        if(different priorities among objectives)
            Modify the ranks in favour of the objective with preference;
        Select individuals for reproduction on basis of rank;
        Recombine the selected individuals employing crossover and mutation operators;
    }
    Evaluate P(t+1);
    t:=t+1;
until termination condition is met
```

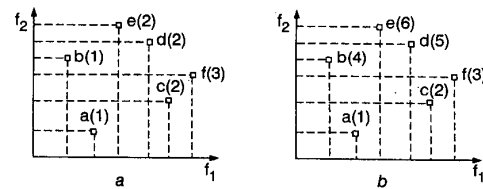**Fig. 10** *Flowchart of proposed GA for multiobjective optimisation*

7.4 Variable recombination operators

In a typical GA, the crossover and mutation operators are the most important components that influence the GA's efficiency to give maximum exploration of the search space, and ensure convergence towards global optima. To attain the best GA performance, the crossover probability is assigned a large value at the beginning of the optimisation and linearly reduced in subsequent generations. The mutation probability is varied in the opposite direction.

IEE Proc.-Electr. Power Appl., Vol. 146, No. 5, September 1999

575

7.5 Treatment of preferred priorities among objectives

In practice, the decision-maker may wish to optimise certain objectives, and the proposed approach should allow such a preference. The above rank assignment method is modified as in the two-objective minimisation example of Fig. 11b. Fig. 11a shows the rank assignment for 6 candidate solutions, where equal priorities are placed between the minimising objective f_1 and the minimising objective f_2. Both solutions a and b are ranked as level 1 since $f_1(a) > f_1(b)$ but $f_2(a) < f_2(b)$. Likewise, solutions c, d and e are ranked as level 2 and solution f is ranked as level 3. Should the decision-maker wish to give a higher priority to minimising the objective f_2 than to minimising the objective f_1, candidate solutions a, c and f are ranked at a higher level

(more successful) than candidate solutions b, d and e. Candidate solutions a, c and f will thus be selected for reproduction, and will have a higher probability of survival in subsequent generations.

Fig. 11 Rank assignments for different priorities among objectives
a f_2 has the same priority as f_1
b f_2 has greater priority than f_1

576

IEE Proc.-Electr. Power Appl., Vol. 146, No. 5, September 1999